Image Recognition of Shape Defects in Hot Steel Rolling

Evgeniya Balmashnova (Eindhoven University of Technology), Mark Bruurmijn (Eindhoven University of Technology), Ranjan Dissanayake (Rajarata University), Remco Duits (Eindhoven University of Technology), Mark Bruurmijn (Eindhoven University of Technology), Leo Kampmeijer (Tata Steel Research Development and Technology), Tycho van Noorden (Universität Erlangen-Nürnberg)

Abstract

A frequently occurring issue in hot rolling of steel is so-called tail pinching. Prominent features of a pinched tail are ripple-like defects and a pointed tail. In this report two algorithms are presented to detect those features accurately in 2D gray scale images of steel strips. The two ripple detectors are based on the second order Gaussian derivative and the Gabor transform, a localized Fourier transform, yielding the so-called rippleness measures. Additionally a parameter called tail length is defined which indicates to what extent the overall shape of the tail deviates from an ideal rectangular shape. These methods are tested on images from the surface inspection system at Tata Hot Strip Mill 2 in IJmuiden, it is shown that by defining a simple criterion in the feature space spanned by these two parameters a given set of strips can correctly be classified into pinched and non-pinched strips. These promising results open the way for the development of an automatic pinch detection system.

Keywords: Image analysis, Gabor transform, Gaussian scale space.

1 Introduction

One of the key installations on the IJmuiden steel production site is the hot strip mill. In this mill slabs with a length of between 5.5 and 12 m and a thickness of 225 mm, weighing between 8 and 34 tons, are heated up to a temperature of 1200 °C. Along a trajectory of about half a kilometer they are rolled in consecutive steps into strips of up to 2 km long and 2 mm thin. After the final reduction step they are cooled to a temperature in roughly the range 550-750 °C and coiled in generally less than 60 seconds. In this way 250 000 coils leave the hot strip mill each year for further processing and finally end up in construction, in lifting and excavating machines, in consumer goods such as white goods (refrigerators and stoves) and in the automotive and packaging industries.

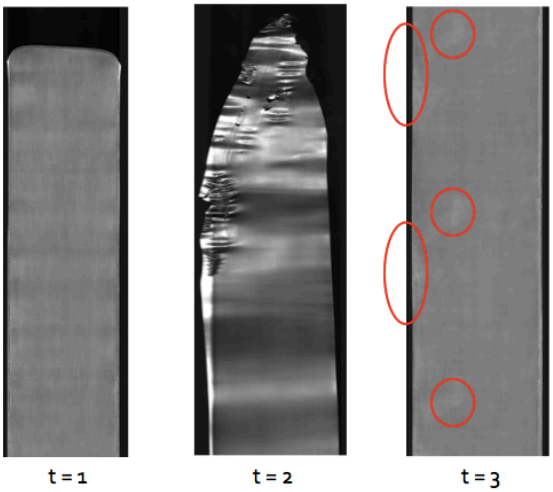

Figure 1: Pictures of parts of three consecutive strips. The first strip ($t = 1$) is without defects, the second strip ($t = 2$) is pinched and has damaged one of the mill rolls which is visible by the periodically occurring defects indicated on the next strip ($t = 3$).

The final reduction steps, where the strips can reach a speed over 20 m/s, are very critical. Errors in the gap settings of the mill may lead to defects in the shape of the strip. Especially at tailing out of the strip such shape defects may lead to pinches, damaging the strip as well as the rolls (see Figure 1), which then in turn need to be changed at significant costs.

Tail pinching is clearly visible by ripples in the strip and the pointed tail. In some case the strip surface is torn apart. It is not exactly known in what circumstances such pinches occur. To determine a statistical relation, and ultimately a causal relation, between certain process conditions and pinching, it is very useful to detect these pinches automatically. Once the mechanism is better understood, an online detection system might also be used to modify the process in order to prevent more pinches.

By means of a camera of the hot strip mill automatic surface inspection system, images of the strip tails are produced. In some of these images pinching is clearly visible. Automatic detection, however, is still problematic. Commercially available surface inspection systems need to be trained with categorized images. Once trained such a system computes the likelihood that a certain defect corresponds to a certain category on the basis of for example their dimensions, orientation on the strip surface and the gray scale distribution. In this way simple defects can be detected quite successfully. However, those systems are not able to detect complex defects such as tail pinches.

The goal of the assignment at hand is to create a method or algorithm that with a large collective of gray scale images can determine for individual strips:

- whether tail pinching has occurred or not;
- the location of the pinches relative to the image frame.

One of the challenges of this problem is that it is difficult to distinguish pinches from other ripple-like defects. It may even be that such shape defects and pinches occur simultaneously.

In this paper we show that for a given collection of strips it is possible to detect tail pinching successfully by considering the overall shape of the tail in combination with the presence of ripples with a certain wave length (Figure 2). For this purpose we have developed three different image analysis techniques to a collection of gray scale images of strip tails. First, we preprocess the images as discussed in Section 2. Subsequently, in Section 3.1, a simple technique, which proofs to be very effective, for estimating the tail shape counting background pixels is explained in more detail. For the detection of ripples we discuss two different methods in Sections 3.2.1 and 3.2.2. For both methods we make use of the fact that the ripples on the strips are always aligned horizontally. The first method tries to find the local maxima caused by the ripples in the vertical direction by looking at second order Gaussian derivatives [3] in that direction. The convolution kernel that is used to compute these second order derivatives contains a scale parameter that can be used to select a length scale at which the derivative information is computed and can be set using the expected bandwidth of frequencies at which the ripples occur. The second, alternative ripple detection method extracts local frequency information from horizontally averaged vertical bands of the images using a Gabor transform [1], which is a localized Fourier transform. Ripples are considered to be spots where high local frequencies are present, which can be assessed using the Gabor transform. In Section 4, we apply the introduced techniques to a collection of images of strip tails and we assess the effectiveness of the techniques for classification purposes. We build a feature space from the extracted features, which can then be used to to classify images into two useful categories. We end this paper in Section 5 with conclusions and recommendations.

2 Preprocessing

The upper image row is removed because it often contains gray artifacts. Since the images taken by the installed camera system are very large (around 8000×2000 pixels), we resize them to 10% of the original sizes (800×200). This allows us to speed up the process without loosing important features since in the rescaled images all the defects are still visible. Background is defined by setting a threshold. For the images we have set this threshold T to 0.15.

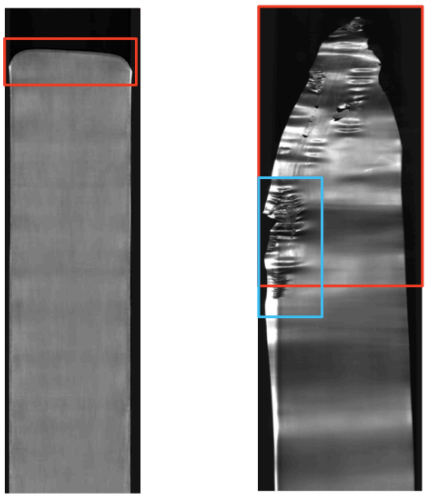

Figure 2: A strip without defects (left) and a pinched strip (right). The techniques discussed in this paper are designed to extract two features: the tail length, indicated by the red rectangles and the appearance of ripples, indicated in blue.

Note that we often consider an image as a continuous function in real space $\mathbb{R}^2$, and therefore we are able to integrate and differentiate. Since in reality we deal with discrete images, the integration is replaced with summation in the implementation of the discussed image analysis techniques.

3 Features

The aim of this project is to find features distinguishing pinched and normal strips. In this report we focus on two which we think are the most important ones - tail length and the presence of high frequency ripples.

3.1 Tail length

One of the main differences between normal and pinched strips is their tail shape. The normal ones have a more square shaped tail and the pinched ones have in most cases an elongated tail (see Figure 2). In order to distinguish these two basic shapes we introduce the parameter *tail length* defined as the distance between the top point of the tail and the place where strip reaches its full width. In order to find this length we compute number of background (black) pixels for each image row in the image. In the lower half of each image normally the width of the strips is almost constant and therefore we estimate from the lower half of

the image the full strip width R by taking the median value of the width in this part of the image (the median is less sensitive to outliers than the mean).

We start scanning the image (size $N \times M$) starting from the top row of pixels. Since in the top row all the pixels are black (gray value below T), the number of black pixels will be equal to N, the length of the image in $x-$dimension. The first row with less than N background pixels is the position of the top point of the tail. The position where the width exceeds R for the first time is the end point of the tail, see Figure 3.

1. For each row i count $B(i)$, the number of pixels with value lower than T, for $i = 1, \ldots, M$
2. i_1 - is the first row (from the top) where $B(i) \neq N$
3. i_2 - is the first row where $B(i) < N - R$.
4. Tail length $L := i_2 - i_1$

In some situations, for example when shadows appear in the image, there may be a lot of black pixels inside the strip, which leads to a wrong estimate of the tail length. The way to improve this feature is to compute the width for each row. By width we mean the distance between the first and the last point with nonzero (non-black) value in an image row. The rest of the procedure is the same. For most of the images it yields the same length (see Figure 4), but for some, with a lot of shadows, the second approach gives more accurate results (see Figure 5).

Although the second approach is more accurate and will be used as a feature for distinguishing between normal and pinched strips, the first approach still has some potential. For example, the difference between two approaches to estimate the tail length, based on the width and the number of non-black pixels, can be used for detecting strips with shadows or holes.

3.2 Rippleness

Tail length alone cannot completely separate pinched and good strips since there are cases when a strip has a normal shape but due to ripples is called a pinched one and there are cases then tail estimation algorithm fails due to shading, see Figure 6. Another feature that distinguishes between normal and pinched strips is the appearance of ripples with high frequency, which mainly occur on pinched strips. We would like to construct a measure of *rippleness* as well as to detect their locations. Ripples are characterized by fast periodic changes of gray-values in vertical direction.

3.2.1 Gaussian derivative

Fast changes of gray values lead to high second order derivative in vertical direction. Derivatives can be computed in a well-defined and well-posed way by using

scale space theory [3] Given a two-dimensional image f, $f : \mathbb{R}^2 \to \mathbb{R}$, its scale representation $u : \mathbb{R}^2 \times \mathbb{R}^+ \to \mathbb{R}$ is defined by the convolution product

$$u(\mathbf{x}, \sigma) = (g(\cdot, \sigma) * f)(\mathbf{x}) \ , \tag{1}$$

in which g is the Gaussian kernel given by

$$g(\mathbf{x}, \sigma) = \frac{1}{2\sigma^2\pi} \exp(-\|\mathbf{x}\|^2/2\sigma^2) \ . \tag{2}$$

Scale space theory allows one to interchange differentiation and convolution, viz. as follows:

$$\partial^\alpha (f * g(\cdot, \sigma))(\mathbf{x}) = (f * \partial^\alpha g(\cdot, \sigma))(\mathbf{x}) \ . \tag{3}$$

This property allows implementation to be fast and robust. We compute the second order Gaussian derivative in$y$-direction $u_{yy}(\mathbf{x}, \sigma)$ with reflective boundary conditions [2]. By choosing the scale σ we can actually tune to the frequencies we are interested in. A maximum filter is applied to the resulting two-dimensional Gaussian derived image, replacing every value by the maximum pixel value in a chosen neighbourhood (in our case 5 pixels).

In order to introduce a measure for the amount of vertical variation for the whole image, we compute the area in the image where the response is higher than some threshold (in our case 0.03). A drawback of this method is that the Gaussian derivative gives a response to any changes, not only periodic ones, therefore edges also give high values. However, the difference between those two is that edges occupy a small area compared to ripples. Images with ripples will have a larger area with responses above the threshold As can be seen from Figure 7 this gives a clear distinction between rippled and flat strips. In the next section we consider another approach, in which frequencies are taken into account in a more explicit fashion, namely the Gabor transform approach.

3.2.2 The Gabor transform

Because ripples occur only locally, the Fourier transform of an image does not not give a clear peak at the frequency of the ripples, i.e. detection is practically impossible. This is directly related to the fact that the ripples are local. The Gabor transform [1] is a windowed-Fourier transform, which is well suited to find local frequencies. We restrict ourself to the one-dimensional case, since we are looking for harmonic behavior in the vertical direction only. Applying the two-dimensional Gabor transform to the whole image is computationally too heavy. Therefore we cut the images into K bands (we used 20 for the visualization purposes, but it can be less), and for each band we construct a one-dimensional intensity profile f_i, $k \in [1, \ldots, K]$ by summing up all values in every row.

Continuous case Although images are always discrete, the theory we use is for the continuous case. Later we will translate it to the discrete case. The Gabor

transform $G_\psi(f) : \mathbb{R} \times \mathbb{R} \to \mathbb{C}$ of a signal $f \in \mathbb{L}_2(\mathbb{R})$ is given by

$$G_\psi(f)(y, \omega) = \int f(\xi)\overline{\psi(y - \xi)}e^{-2\pi i(y-\xi)\omega}\mathrm{d}\xi \,, \tag{4}$$

where ψ is the Gaussian kernel in $1D$,

$$\psi(y) = \frac{1}{2\sigma^2\pi}\exp(-y^2/2\sigma^2) \,. \tag{5}$$

The Gabor transform yields a complex-valued spectrum in each spatial position, which can now be used to find positions in which high frequencies are present (i.e. ripples). However, we are not interested in the phase of the frequency pattern, but only in its amplitude. Therefore, we define the probability density function of finding a certain frequency ω at position y as:

$$U_k(y, \omega) = |G_\psi(f_k)(y, \omega)|^2, \; k = 1, \ldots, K \,. \tag{6}$$

Discrete case For the images vertical coordinate y takes only integer values, $y \in [1, \ldots, M]$ and 4 has a summation instead of integration

$$U_k(y, \omega) = \left| \sum_{k=0}^{M} f(k)\overline{\psi(y - k)}e^{-2\pi i(y-k)\omega} \right|^2 , \tag{7}$$

$\omega \in [-M/2, \ldots, \ldots, M/2]$. Due to the symmetry around zero, for the computation it is enough to consider only positive side of the spectrum. Locations with ripples differ from normal ones by giving high response for certain ω values (Figure 8).

We define the first moment by

$$E_k(y) = \sum_{\omega=0}^{M/2} U_k(y, \omega)\omega, \; k = 1, \ldots, K \,. \tag{8}$$

It gives larger weight to high frequencies and allows to filter zero frequency response in a soft way. The first moment for locations in a flat area will be close to zero, since only frequencies in the neighborhood of zero are present. For a rippled area the first moment will be shifted to a higher value (Figure 9). Therefore the first moment is expected to be a reasonable measure of rippleness. We use the total response $\sum_{k=1}^{K}\sum_{y=1}^{M} E_k(y)$, where we sum over every cut band, of an image as a measure of severeness of the ripple defects.

4 Classification

We have discussed two measures: tail length and rippleness. For rippleness we introduced two methods, which are highly correlated and it is subject for further

experiments to decide which one is more favorable for classification purposes (we use the Gaussian derivative for further experiments in this paper). Note that both methods have their advantages. For example, the Gaussian derivative requires less computational power but with the Gabor transform specific frequencies can be detected. In Figure 10 a two-dimensional feature space is presented. As one can see, the defected strips (green dots) are, as expected, more scattered in feature space. The straight line in the figure represents a possible and simple manner to classify the images of the strips into two classes: normal strips and strips with a defect. We have a set of images with labels "normal" and "pinched", with 163 normal and 21 pinched strips. For the labeled training set we take the line $y = ax + b$ (for the collection we have $y = 8000 - \frac{8000}{125}x$) that separates the most normal strips (96.3% are true negative) from strips with a defect (for the 3.6% false positive results, see Figure 11), without creating false negatives (0% false negative). The classification has not been considered thoroughly and may be improved further. For new cases the decision is taken by determining on which side of the line the image is in feature space. We would like to stress that, apart from classification use, the introduced features could also indicate severeness of the pinching as shown in Figure 12-13.

5 Conclusions and recommendations

In this paper features of two different types have been considered: the tail length and the presence of ripples. For each of them two different approaches are given and compared. Although all of them have some advantages, only one of each type was chosen for the classification (the tail length based on width estimation and rippleness using Gaussian derivatives), and a simple, but effective, classification rule has been considered. As a result we have constructed an efficient algorithm with which one can:

- distinguish tail shape;
- detect and locate ripples;
- effectively classify pinching.

We propose several points for further research:

1. Based on the proposed features, a measure of severeness of the defect can be introduced.
2. Improvement of existing features can be done:
    - In the Gabor domain the important information is hidden by fluctuations. Applying (contextual) enhancements in the Gabor domain before extracting features such as the 1st order moment Equation (8) can clean up the signal and improve the results;

- Rippleness measure requires some parameters, like scale for the Gaussian window. It is an open question whether just one scale should be fixed, or several of them can bring more information. Therefore rippleness can be extended to a multi-scale framework: edge focussing, automatic scale selections, tracking critical path of the Laplacian in scale space.

3. Consider other features in the Gabor domain, e.g. other moments or responses to the certain range of frequencies, corresponding to the bandwidth of the actual ripples (this would correspond to changing the summation limits in Equation 8 on $[\omega_0, \omega_1]$, where the limit values are obtained from statistics of ripple frequencies).

4. Classification in feature space should be explored further. A basic linear discriminant analysis (as in Sec. 4) would probably be sufficient.

5. New features can be introduced:

   - Deformation modeling. Unfortunately, the process does not allow imaging of an evolving process. So use idealized flat image as reference for rough single step deformation estimates. The amount of deformation needed to obtain the image from the ideal can tell about the severeness of the defect.
   - 2D-filtering to detect endings of ripples and scratches.
   - Include contextual filters via the Gabor domain. It is important to check whether the surrounding local frequencies are coherent/aligned or not. This could distinguish between folding and ripples. If some frequency appear over the complete x-axis than it is a fold and it can be filtered out.
   - New applications. Ripple detection algorithms are developed in this work can also be applied to other wave-like shape defects over other parts of the strip, and hence can be used to distinguish wavy edges, quarter buckles and center buckles much more accurately than with the standard optical shape meter at the hot strip mill.

References

[1] D. Gabor. Theory of communication. part 1: The analysis of information. *Journal of the Institution of Electrical Engineers - Part III: Radio and Communication Engineering*, 93(26):429–441, november 1946. doi: 10.1049/ji-3-2.1946.0074.

[2] B. M. t. Haar Romeny. *Front-End Vision and Multi-Scale Image Analysis: Multi-Scale Computer Vision Theory and Applications, written in Mathematica*, volume 27 of *Computational Imaging and Vision Series*. Kluwer Academic Publishers, Dordrecht, The Netherlands, 2003. ISBN 1-4020-1507-0.

[3] T. Lindeberg. On the axiomatic foundations of linear scale-space. In J. Sporring, M. Nielsen, L. M. J. Florack, and P. Johansen, editors, *Gaussian Scale-Space Theory*, volume 8 of *Computational Imaging and Vision Series*, chapter 6, pages 75–97. Kluwer Academic Publishers, Dordrecht, The Netherlands, 1997.

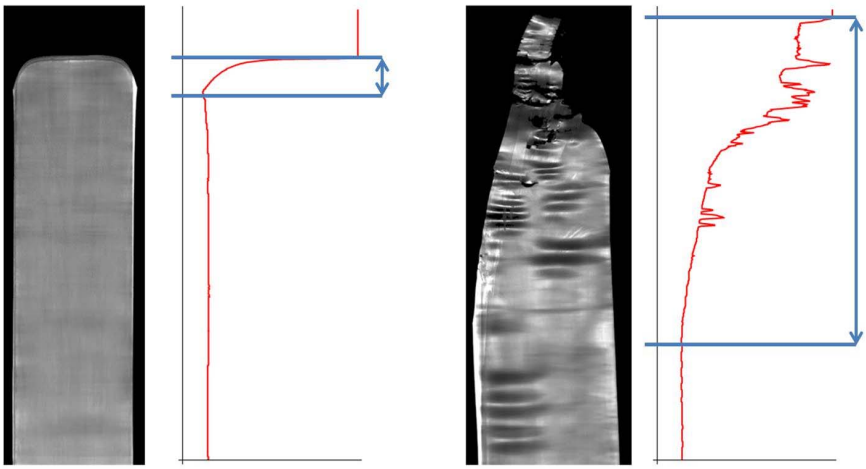

Figure 3: Tail length estimation for a strip without defects (left) and a pinched strip (right): red graph represents number of background pixels per row.

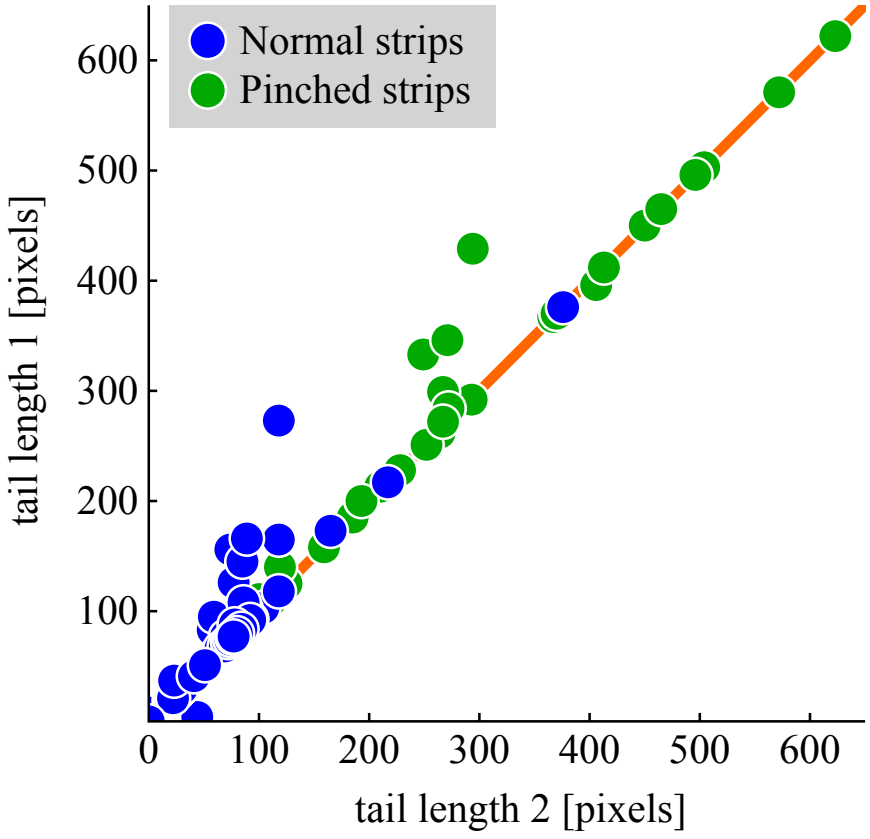

Figure 4: Two different tail length estimations, based on width estimation on x-axis and based on black pixels on the y-axis. Green dots represent pinched strips and blue dots normal strips.

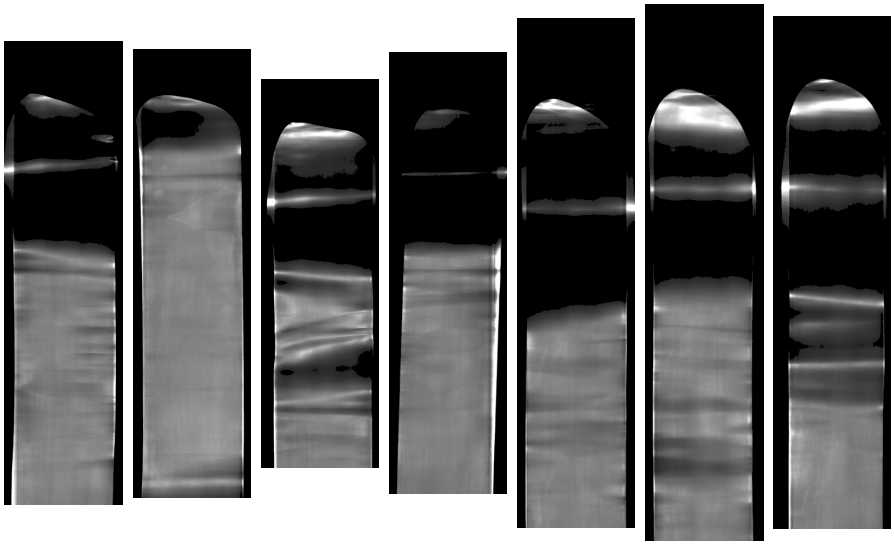

Figure 5: Cases when computing width directly leads to better tail length estimation.

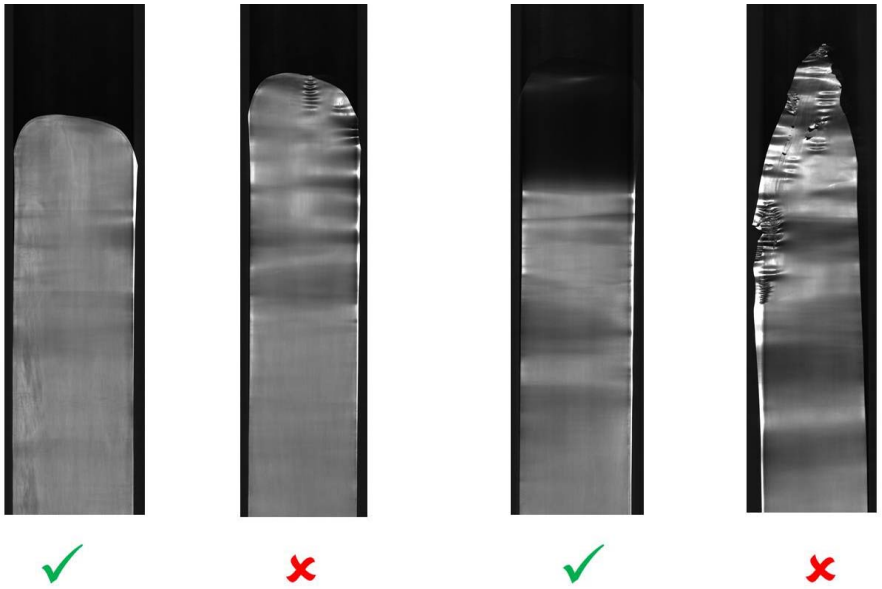

Figure 6: Tail length fails to separate pinched strips from the rest.

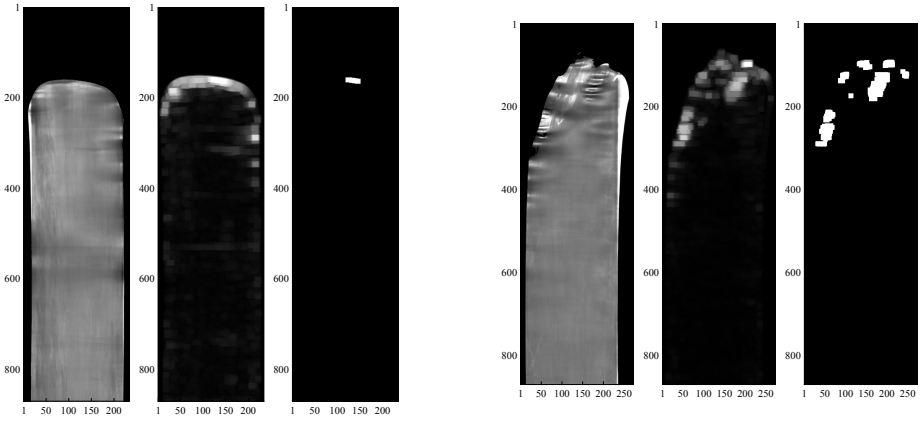

Figure 7: Results (before and after thresholding) of applying the Gaussian derivative to normal (left) and to pinched (right) strips.

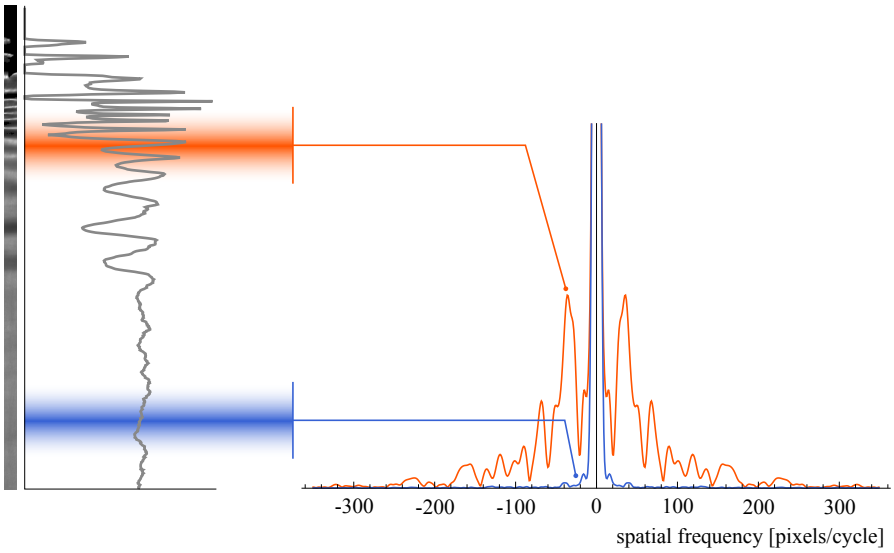

Figure 8: Left: band cut from pinched strip image (870×27 pixels) and its intensity profile by summing over rows. Right: local spectra from the two indicated regions in the intensity profile. The rippled region (orange) contains more high frequencies than the flat region (blue).

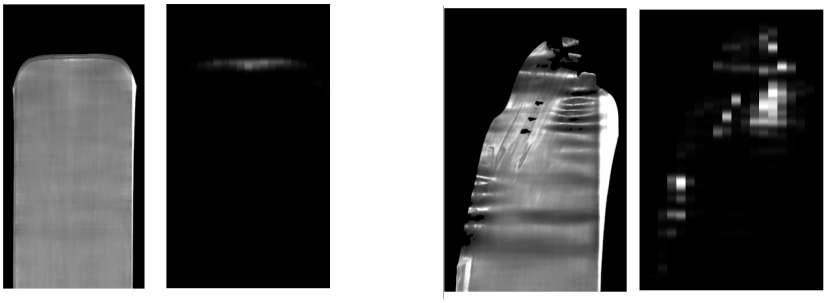

Figure 9: The first moment for a normal and a pinched strips.

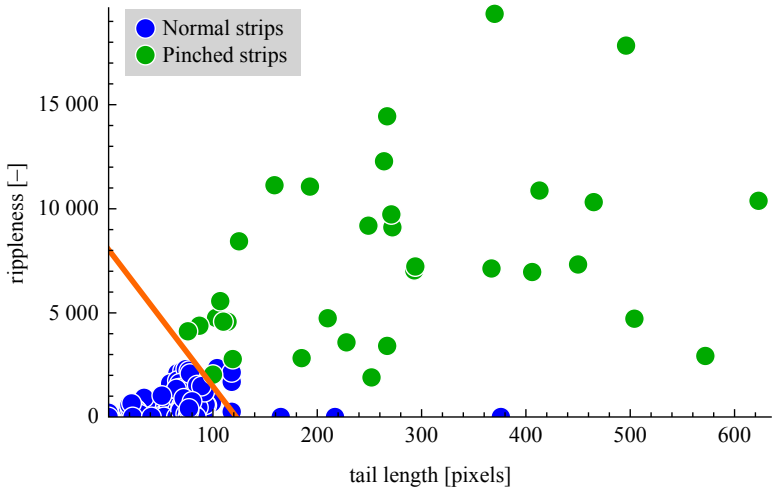

Figure 10: Feature space, tail length on x-axis and rippleness (using Gaussian derivatives) on y-axis. Green dots represent pinched strips and blue ones normal strips.

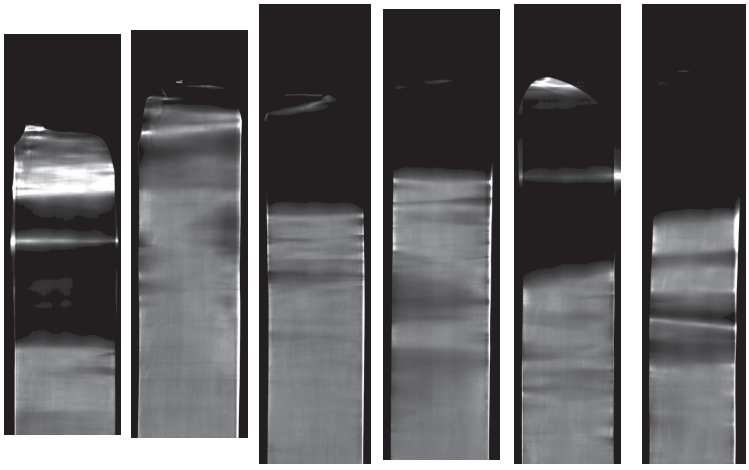

Figure 11: False positive classification results.

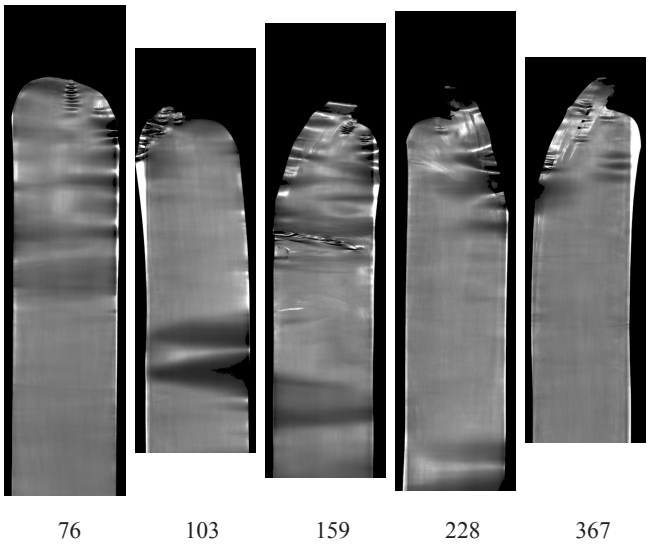

Figure 12: Pinched strips sorted according to their tail length.

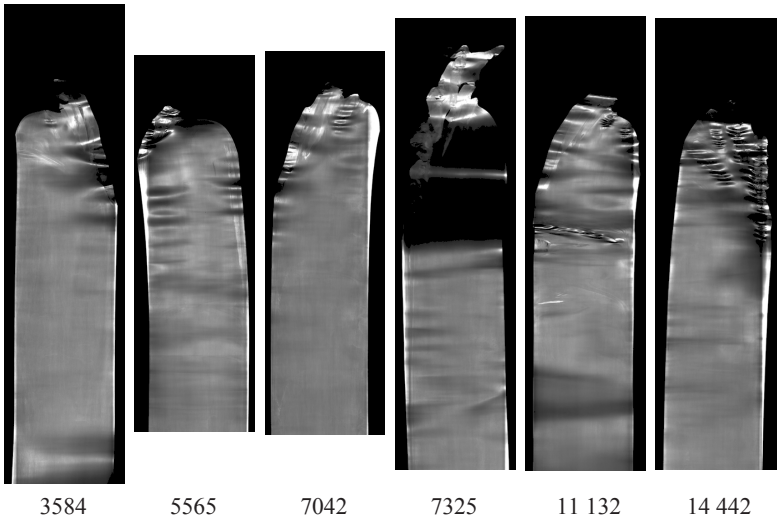

Figure 13: Pinched strips sorted according to the severeness of their ripples.